

Abscinazole-E2B, a practical and selective inhibitor of ABA 8'-hydroxylase CYP707A

メタデータ	言語: eng 出版者: 公開日: 2012-06-28 キーワード (Ja): キーワード (En): 作成者: Okazaki, Mariko, Kittikorn, Monrudee, Ueno, Kotomi, Mizutani, Masaharu, Hirai, Nobuhiro, Kondo, Satoru, Ohnishi, Toshiyuki, Todoroki, Yasushi メールアドレス: 所属:
URL	http://hdl.handle.net/10297/6728

Abscinazole-E2B, a practical and selective inhibitor of ABA 8'-hydroxylase CYP707A

Mariko Okazaki^{a,†}, Monrudee Kittikorn^{b,†}, Kotomi Ueno^c, Masaharu Mizutani^c, Nobuhiro Hirai^d, Satoru Kondo^b, Toshiyuki Ohnishi^e, Yasushi Todoroki^{a,*}

^a *Department of Applied Biological Chemistry, Faculty of Agriculture, Shizuoka University, Shizuoka 422-8529, Japan*

^b *Division of Bioresource Science, Graduate School of Horticulture, Chiba University, Matsudo 271-8510, Japan*

^c *Graduate School of Agricultural Science, Kobe University, Kobe 657-8501, Japan*

^d *Division of Environmental Science and Technology, Graduate School of Agriculture, Kyoto University, Kyoto 606-8501, Japan*

^e *Division of Global Research Leaders, Shizuoka University, Shizuoka 422-8529, Japan.*

Keywords: Plant growth regulator, P450 inhibitor, ABA

* Corresponding author. Tel./fax: +81 54 238 4871.

E-mail address: aytodor@ipc.shizuoka.ac.jp (Y. Todoroki)

† These authors contributed equally to this work.

ABSTRACT

We developed abscinazole-E2B (Abz-E2B), a practical and specific inhibitor of abscisic acid (ABA) 8'-hydroxylase (CYP707A), by structural modification of abscinazole-E1 (Abz-E1), another compound we developed. A butoxy group was introduced to Abz-E2B instead of the tosylate group of Abz-E1, in expectation of better water solubility, because the calculated log *P* value of Abz-E2B is 3.47, which is smaller than that of Abz-E1 (4.02). The water solubility of Abz-E2B was greater than 90% at a concentration of 100 μ M, at which the solubility of Abz-E1 was 20%. The enzyme specificity was improved significantly. In *in vitro* assays constructed using recombinant enzymes, (\pm)-Abz-E2B was a considerably weaker inhibitor than (\pm)-Abz-E1 for CYP701A, a GA biosynthetic enzyme, which is a target of *S*-uniconazole (*S*-UNI), a lead compound of Abz-E1. (\pm)-Abz-E2B application to plants resulted in improved desiccation tolerance and an increase in endogenous ABA, with little retardation of growth. We also prepared optically pure Abz-E2B and determined its absolute configuration. The *R*-enantiomer of Abz-E2B was the more potent inhibitor of CYP707A, unlike UNI, whereas both enantiomers were markedly less effective than *S*-UNI in inhibiting CYP701A. Because *S*-Abz-E2B arrested the growth of rice seedlings at 100 μ M, probably because of off-target effects, *R*-Abz-E2B should be used as a chemical tool for research focusing on CYP707A when 100 μ M or higher concentration is required, although (\pm)-Abz-E2B may be useful as an alternative option at a lower concentration.

1. Introduction

The plant hormone abscisic acid (ABA) is involved in seed dormancy, stress responses, and other physiological events.¹⁻⁴ Its biosynthesis, transport, and catabolic inactivation cooperatively regulate the endogenous level of ABA in response to environmental changes.¹⁻⁴ A chemical compound that perturbs this highly controlled system is promising as a chemical probe for the mechanism of ABA action.⁵ In addition, this chemical is potentially useful in agriculture and horticulture. Although ABA is registered as an agricultural farm chemical (plant growth regulator), its practical use has been limited, mainly due to its weak effect in field trials,⁶ considered to be due to its rapid inactivation through biodegradation. Catabolic inactivation of ABA is mainly controlled by ABA 8'-hydroxylase, a member of the CYP707A subfamily, which is the cytochrome P450 catalyzing the C8'-hydroxylation of ABA to 8'-hydroxy-ABA (Fig. 1) and its more stable tautomer, phaseic acid, which has considerably lower hormonal activity than ABA.^{4,7,8-14} Thus, we have focused on developing a specific inhibitor of ABA 8'-hydroxylase.

The plant growth retardant *S*-uniconazole (*S*-UNI)^{15,16} functions as an inhibitor of CYP707A¹⁷ in addition to *ent*-kaurene oxidase (CYP701A), which catalyzes the three-step oxidation of *ent*-kaurene to *ent*-kaurenoic acid (KA),¹⁸ a biosynthetic precursor of the plant hormone gibberellin (GA). *S*-Diniconazole, the *R* enantiomer of which is a fungicide with a structure very similar to *S*-UNI, also inhibits CYP707A,¹⁹ although it arrests plant growth.²⁰ The broad inhibition spectrum of some azole compounds against P450 enzymes has apparently resulted from the heme coordination of an azole nitrogen, which is a common mechanism of azole P450 inhibitors. In other words, their specificity for individual P450 enzymes depends on structural properties other than the azole group.

In early work,²¹ we modified the structure of *S*-UNI to develop a more specific inhibitor against CYP707A by various approaches.²²⁻²⁴ The molecular enlargement approach, which was the most effective, led us to develop a specific inhibitor of CYP707A, (±)-UTn.²² However, Because (±)-UTn was difficult to dissolve in water because of its high

hydrophobicity, it was difficult to handle as a chemical tool. Aiming to overcome this defect, we developed (\pm)-abscinazole-E1 (Abz-E1, Fig. 1), which has a tosylate-protected diethylene glycol chain instead of an alkyl chain.²⁵ This compound has better water solubility than (\pm)-UT n . However, its water solubility was still lower than that of *S*-UNI. Moreover, because the tosylate group is chemically reactive and rich in intermolecular interactions, (\pm)-Abz-E1 is not practical enough for both research and agricultural uses, although it may be useful as a precursor for structural evolution. In the present study, therefore, we improved the chemical and biological properties of (\pm)-Abz-E1 to develop a more practical and specific inhibitor of CYP707A. We describe the design and preparation of a novel CYP707A inhibitor, abscinazole-E2B (Abz-E2B, Fig. 1), its water solubility, and its effect on CYP707A and CYP701A both in vitro and in vivo. We also describe the preparation, absolute configuration, and enzymatic and biological effects of optically pure Abz-E2B.

2. Results and Discussion

(\pm)-UT n (Fig. 1), an enlarged analogue of *S*-UNI, has a 4-alkyl-1,2,3-triazole instead of the chlorine of *S*-UNI. Our previous study showed that a longer alkyl chain results in higher inhibitory activity for CYP707A and lower for CYP701A.²² However, the longer alkyl chain encourages hydrophobicity. In fact, (\pm)-UT n ($n > 4$) with the longer carbon chain is unable to dissolve in water in the concentration range required for bioassays (1-100 μ M), although it can be partially dissolved in buffer solution at concentrations required for enzyme assays (1-100 nM). On the other hand, the introduction of protic functional groups in the alkyl chain diminishes the inhibitory activity. Thus, we developed (\pm)-Abz-E1, which has a tosylate-protected diethylene glycol chain.²⁵ The inhibition constant (K_i) of (\pm)-Abz-E1 for recombinant *Arabidopsis* CYP707A3 co-expressed with *Arabidopsis* P450 reductase (ATR2) in *Escherichia coli* was 27 nM,²⁵ which was considerably smaller than that of (\pm)-UT4 (195 nM). This improved activity was considered to result from either the long chain, ether linkage, or tosylate moiety. Especially because a tosylate moiety is large and rich in intermolecular

interactions, we first tried to detosylate (\pm)-Abz-E1 to evaluate the effect of the tosylate moiety on inhibition of CYP707A.

Treatment of (\pm)-Abz-E1 with lithium aluminum hydride in THF at room temperature gave two products (Scheme 1). One is the detosylated compound **1**, and the other is the more reduced compound **2**. The K_I values of **1** and **2** for recombinant *Arabidopsis* CYP707A3 were 850 and 270 nM, respectively, meaning that these compounds have lower affinity for the CYP707A3 active site than Abz-E1. This suggests that the tosylate moiety of Abz-E1 plays a significant role in binding to the CYP707A3 active site. However, other possibilities are not excluded. Compound **1** has a terminal hydroxy group, and the chains of both compounds **1** and **2** are shorter than that of Abz-E1. Because the introduction of protic functional groups in the alkyl chain of (\pm)-UT n diminished the inhibitory activity and CYP707A3 preferred binding to UT n with the longer alkyl chain, these structural properties of compounds **1** and **2** may reduce the affinity for the CYP707A3 active site. To evaluate the effect of the tosylate group of Abz-E1, we had to create new compounds that have a longer chain with no hydroxy group. Accordingly, we designed abscinazole-E2P and abscinazole-E2B (Fig. 1), which respectively have a propoxy and butoxy group instead of a tosylate, considering that both the length of the chain and the calculated log P value, which should be less than 3.5 for better water solubility than Abz-E1 (calculated log P = 4.02).

(\pm)-Abz-E2P and (\pm)-Abz-E2B were prepared from (\pm)-Abz-E1 by treatment with sodium hydride in propanol and butanol, respectively (Scheme 2). The K_I values for recombinant *Arabidopsis* CYP707A3 were 130 nM for (\pm)-Abz-E2P and 36 nM for (\pm)-Abz-E2B. This means that the affinity of Abz-E2B for the CYP707A3 active site is nearly equivalent to that of Abz-E1 (K_I = 27 nM). Therefore, the tosylate moiety of Abz-E1 seems not to be essential for the high affinity to the active site. Considering that (\pm)-Abz-E2B was more potent than (\pm)-Abz-E2P, the factors responsible for the high activity of (\pm)-Abz-E1 are not specific π - π , CH- π , or electrostatic interactions by the tosylate moiety but nonspecific hydrophobic interaction of the terminal lipophilic moiety with the lipophilic region at the active site.

The water solubility of (±)-Abz-E2P and (±)-Abz-E2B was more than 90% at a concentration of 100 µM, whereas it was 20% for (±)-Abz-E1 and 40% for S-UNI under the same conditions (Table 1), meaning that these new compounds, especially Abz-E2B, are ideal CYP707A inhibitors with both potent activity and good water solubility.

We examined the selectivity between CYP707A and CYP701A by evaluating both inhibitory activity against recombinant rice CYP701A6 expressed in insect cells using a baculovirus vector and growth of rice seedlings. Because CYP701A enzymes catalyze all three steps to KA via the corresponding alcohol and aldehyde,¹⁸ we evaluated the IC₅₀ value for formation of the end product, KA, instead of the *K_I* value, which requires very complicated kinetic analysis. We were unable to determine the IC₅₀ values of (±)-Abz-E2P and (±)-Abz-E2B because 50% inhibition was not achieved even at the highest tested concentration, 1 µM, when 1 µM of the substrate *ent*-kaurene was used, whereas the IC₅₀ values of Abz-E1 and UNI were 1 µM and 57 nM under the same conditions (Table 1). This result, together with the strong effect on CYP707A, suggests that the CYP707A/CYP701A selectivity of Abz-E2P and Abz-E2B is considerably higher than that of Abz-E1. On the other hand, slight inhibition of rice seedling growth by (±)-Abz-E2P and (±)-Abz-E2B was observed only at a high concentration, 100 µM (Fig. 2). This was the same trend observed for (±)-Abz-E1, although, based on the very weak in vitro inhibition of CYP701A, the growth retardant effect of (±)-Abz-E2P and (±)-Abz-E2B is expected to be considerably smaller than that of (±)-Abz-E1. The inhibitory profiles in the in vitro enzyme assay using the recombinant enzyme may not fully correspond to those in the in vivo enzyme reaction. Otherwise, the observed inhibition of growth may depend on inhibition of CYP707A to increase endogenous ABA, or on inhibition of off-target enzymes other than CYP701A and CYP707A. This question is discussed again below.

The effect of (±)-Abz-E2P and (±)-Abz-E2B on seed germination and early growth of lettuce was examined in both the presence and absence of ABA (Fig. 3a and 3b). In the absence of ABA, neither compound had an effect at a concentration of 100 µM. On the other hand, in the presence of ABA, they enhanced the effect of ABA. The effect of (±)-Abz-E2P

was slight in the presence of 3 μM ABA and significant in the presence of 10 μM ABA, whereas that of (\pm)-Abz-E2B was slight in the presence of 1 μM ABA and significant in the presence of 3 and 10 μM ABA. The greater effect of (\pm)-Abz-E2B than (\pm)-Abz-E2P was consistent with results of in vitro CYP707A3 assays. This suggests that the enhancement of ABA activity depends on inhibition of ABA inactivation. We also tested the effect of (\pm)-Abz-E2B on germination and leaf emergence of *Arabidopsis thaliana* in both the presence and absence of ABA. In contrast to the lettuce assay, (\pm)-Abz-E2B exhibited an inhibitory effect at 100 and 300 μM in the absence of ABA. Although this activity may arise from an increase in endogenous ABA due to CYP707A inhibition, it was enhanced less than expected by co-treatment with ABA (Fig. 3c and 3d).

Among the tested plants, the effect of (\pm)-Abz-E2B in the absence of exogenous ABA was the most significant for *Arabidopsis* seeds. Although lettuce seeds and rice seedlings were insensitive to (\pm)-Abz-E2B in the absence of exogenous ABA, the lettuce seeds were more responsive in the presence of ABA. Rice seedlings were so insensitive to (\pm)-Abz-E2B that their early growth was not affected by co-treatment with ABA (data not shown). This difference may depend on a difference in ABA sensitivity, activity and ligand recognition of CYP707A homologues, or sensitivity to residual CYP701A inhibitory activity of (\pm)-Abz-E2B.

We also tested the enhancement of (\pm)-Abz-E2B on desiccation tolerance under more practical conditions. Nineteen-day-old bent grass (*Agrostis capillaris*) was sprayed with an aqueous solution containing (\pm)-Abz-E2B at 50 μM . Water was not supplied for 10 days, and the plants were then rehydrated. Application of (\pm)-Abz-E2B before dehydration induced significant drought tolerance during dehydration (Fig. 4a). The endogenous amount of ABA during dehydration increased significantly at day 9 after treatment with (\pm)-Abz-E2B (Fig. 4b). The increase in ABA content on days 7 to 9 suggests that plants activated ABA biosynthesis by sensing water deficit stress after 7 days. Inhibition of ABA catabolism by Abz-E2B must have increased the ABA content.

In the above-mentioned enzymatic and biological assays, Abz-E2B was applied in racemic form. The *S*-isomer of the parent lead compound UNI is more potent than the *R*-isomer in inhibiting CYP707A. To verify that the selective inhibitory activity of (±)-Abz-E2B for CYP707A is also caused by the *S*-isomer, optically pure Abz-E2B was prepared from optically pure Abz-E1, which was prepared by optical resolution of the racemate using semipreparative HPLC with a chiral column. The absolute stereochemistry of both enantiomers of Abz-E2B was determined by an advanced Mosher's method²⁶ using ¹H NMR spectra of their *R*-α-methoxy-α-(trifluoromethyl)phenyl acetates (MTPA). The *R*-MTPA esters were prepared with *S*-MTPA-Cl in pyridine. For convenience, we prepared MTPA esters of optically pure Abz-E2B by diastereomeric resolution of *R*-MTPA-(±)-Abz-E2B using preparative HPLC with a silica gel column. The rotational sign of Abz-E2B in the diastereomers was identified on the basis of chiral HPLC analysis of Abz-E2B released by hydrolysis of the diastereomers after the ¹H NMR analysis. To exclude the possibility that the MTPA plane is not formed owing to the bulky *t*-butyl group, we constructed a molecular model of the MTPA esters. The geometries, optimized with B3LYP/6-31G(d) from the initial geometries with the ideal MTPA plane, retained the plane sufficiently to apply the advanced Mosher's method, even though the plane was slightly distorted (Figure 5). In addition, we experimentally confirmed that the advanced Mosher's method gave the correct absolute configuration of UNI (see Supplementary data). The phenyl moiety in MTPA is located so as to have a shielding effect on the vinylazole moiety for *S*-Abz-E2B and the *t*-butyl group for *R*-Abz-E2B. ¹H NMR analysis showed that the vinyltriazole protons of the (+)-isomer and the *t*-butyl protons of the (–)-isomer were shielded. Thus, the absolute configuration of the (+)- and (–)-isomers was determined to be *S* and *R*, respectively.

Both enantiomeric isomers of Abz-E2B were assayed enzymatically and biologically. *R*-Abz-E2B was a more effective inhibitor of recombinant *Arabidopsis* CYP707A3 than the *S*-isomer by a factor of 10 on the basis of the K_I values (Table 1). This is inconsistent with the case of UNI, which had an *S*-isomer that was more potent than the *R*-isomer by a factor of

more than 100.²³ The enhancement of exogenous ABA activity on seed germination and early growth of lettuce and *Arabidopsis* showed the same trend. *R*-Abz-E2B enhanced the inhibition of lettuce seed germination and early growth of lettuce and *Arabidopsis* more than *S*-Abz-E2B (Fig. 6a-6d), although neither enantiomer had a significant enhancement of exogenous ABA activity in *Arabidopsis* seed germination, consistent with the case of racemic Abz-E2B (Fig. 3c).

Comparing *S*- and *R*-UNI in the same most stable conformation (**A**), the largest structural difference between them is the relative space occupied by the triazole, especially N4", which would coordinate the heme iron in the CYP707A active site, and the *t*-butyl (Fig. 7). If *R*-UNI adopts a different conformation from *S*-UNI, this steric difference may be considerably canceled. The UNI molecule is relatively flexible, which allows it to adopt at least four specific conformers by rotation of two single bonds, C2-N1" and C2-C3.²⁷ The conformers **B** and **C**, rather than **A**, of *R*-UNI resemble conformer **A** of *S*-UNI in their spatial relationship between N4" and the *t*-butyl (Fig. 7). The theoretical energy difference between **A/B** or **A/C** is respectively calculated to be 2.5 or 4.0 kcal mol⁻¹ in the gas phase, meaning that **B** and **C** are theoretically less advantageous in binding to the CYP707A active site than **A** by a factor of 100-1000, which fluctuates according to interactions with the active site residues. From this point of view, the activity of *R*-UNI, which is lower than *S*-UNI by a factor of 140, may be reasonable, although the **A** conformer of *R*-UNI may merely have lower affinity to the active site than *S*-UNI by a factor of 140. The structure of Abz-E2B is the same as that of UNI except for the 1,2,3-triazole, which possesses a long ether chain. Because the UNI portion in the Abz-E2B molecule must have similar conformational properties to UNI, the remaining portion of the structure must be responsible for the inverted enantiomeric property. The long side chain of *R*-Abz-E2B may interact more effectively with the CYP707A active site than that of *S*-Abz-E2B. Because the length of the side chain of Abz-E2B is comparable to that of the UNI molecule, the energetic contribution to binding the CYP707A active site may be large enough to override the disadvantage of the UNI portion of the *R*-isomer in fitting into the active site. Such an inversion accompanying structural modification of chiral compounds

has also been observed for an ABA analogue, AH11, which functions as an inhibitor of CYP707A.²⁸

Conversely, in the inhibition of rice seedling growth, *S*-Abz-E2B showed slightly stronger average activity than the *R*-isomer at a concentration of 100 μ M (Fig. 8a). The retardant effect of *S*-Abz-E2B at 100 μ M fluctuated, unlike that of the *R*-isomer. Some rice seedlings treated with 100 μ M *S*-Abz-E2B were markedly arrested in growth and were comparable to dwarf seedlings resulting from 30-100 μ M *S*-UNI treatment (Fig. 8b). The rescue by co-treatment with GA₃ and *S*-Abz-E2B was less effective than co-treatment with GA₃ and *S*-UNI (Fig. 9). Considered together with the very low effect of *S*-Abz-E2B on CYP701A, this unusual dwarfing may depend on inhibition of not only CYP701A but also other enzymes. Thus, *R*-Abz-E2B should be used as a chemical tool for research focusing on CYP707A when 100 μ M or higher concentration is required. At a lower concentration than 100 μ M, (\pm)-Abz-E2B may be useful as an alternative option.

3. Conclusions

We developed Abz-E2B, a novel inhibitor of ABA 8'-hydroxylase (CYP707A). Abz-E2B, a structural analogue of UNI that substitutes a 4-(2-(2-butoxyethoxy)ethoxy)methyl-1*H*-1,2,3-triazole for a chlorine, is more specific, chemically stable, and water soluble than Abz-E1, another inhibitor we reported on,²⁵ which has a tosylate instead of the butoxy in Abz-E2B. In an in vitro recombinant P450 inhibition assay, (\pm)-Abz-E2B was more potent against CYP707A3 and less potent against CYP701A6 than (\pm)-Abz-E1. This superior inhibitory specificity of CYP707A was confirmed in bioassays. Bent grass sprayed with (\pm)-Abz-E2B solution exhibited stronger drought tolerance than control grass sprayed with distilled water. The optically active Abz-E2B exhibited different enantiomeric properties from UNI in CYP707A inhibition and related biological assays. The *R*-enantiomer of Abz-E2B was the more potent inhibitor of CYP707A, unlike UNI, whereas the *S*-enantiomer arrested the growth of rice seedlings at high concentration,

probably because of off-target effects. Therefore, *R*-Abz-E2B should be used as a chemical tool for research focusing on CYP707A, although (\pm)-Abz-E2B may be useful as an alternative option at low concentration.

4. Experimental

4.1. General

(+)-ABA was a gift from Toray Industries Inc., Tokyo, Japan. *ent*-Kaurene and *ent*-kaurenoic acid were gifts from Prof. Tomonobu Toyomasu (Yamagata University) and Dr. Shinjiro Yamaguchi (RIKEN Plant Science Center), respectively. *ent*-Kaurenoic acid was also purchased from OlChemIm Ltd., Czech Republic. ^1H NMR spectra were recorded with tetramethylsilane as the internal standard using JEOL JNM-EX270 (270 MHz) and JNM-LA500 (500 MHz) NMR spectrometers. ^{13}C NMR and 2D-correlation NMR experiments were recorded using a JNM-LA500 (500 MHz) NMR spectrometer. High resolution mass spectra were obtained with a JEOL JMS-T100LC AccuTOF mass spectrometer. Column chromatography was performed on silica gel (Wakogel C-200).

4.2. Synthesis of chemicals

4.2.1. (*E*)-1-(4-(4-((2-(2-hydroxyethoxy)ethoxy)methyl)-1*H*-1,2,3-triazol-1-yl)phenyl)-4,4-dimethyl-2-(1*H*-1,2,4-triazol-1-yl)pent-1-en-3-ol (1) and (*E*)-1-(4-(4-((2-ethoxyethoxy)methyl)-1*H*-1,2,3-triazol-1-yl)phenyl)-4,4-dimethyl-2-(1*H*-1,2,4-triazol-1-yl)pent-1-en-3-ol (2)

To a stirred solution of Abz-E1 (100 mg, 168 μmol) and molecular sieves 4A in dry THF (25 mL) was added LiAlH_4 (536 mg, 14.1 mmol) at 0 $^\circ\text{C}$ under Ar. The mixture was stirred for 40 min at the same temperature, and for 3 h at room temperature. After quenched with 1 M HCl at 0 $^\circ\text{C}$, the resulting mixture was extracted with EtOAc (90 mL \times 3). The organic

layer was washed with brine, dried over Na₂SO₄, and concentrated in vacuo. The residual oil was purified by silica gel column chromatography with 0-20% acetone in EtOAc to obtain **1** (17.5 mg, 24%) and **2** (20.0 mg, 28%) as colorless oils. A portion of these samples was further purified for bioassays by HPLC (YMC Hydrosphere C18, 150 × 20 mm, 55% MeOH, 8.0 ml min⁻¹, 254 nm) to obtain 7.7 mg of **1** and 8.8 mg of **2**. **1**: ¹H NMR (270 MHz, acetone-*d*₆): δ 0.71 (9H, s, *t*-butyl), 3.54-3.71 (9H, m, -OCH₂CH₂OCH₂CH₂OH), 4.72 (2H, s, 1,2,3-triazole-CH₂O-), 4.82 (1H, d, *J* = 5.9 Hz, HO-3), 5.23 (1H, d, *J* = 5.9 Hz, H-3), 7.20 (1H, s, H-1), 7.70 and 8.01 (each 2H, m, 1-phenyl), 8.04, 8.59, and 8.88 (each 1H, s, 1,2,4-triazole and 1,2,3-triazole); UV λ_{max} (MeOH) nm (ε): 269.6 (19,000); HRMS (ESI-TOF, positive mode): calcd for C₂₂H₃₀N₆O₄Na [M+Na]⁺ 465.2223, found 465.2227. **2**: ¹H NMR (270 MHz, acetone-*d*₆): δ 0.71 (9H, s, *t*-butyl), 1.14 (3H, t, *J* = 6.9 Hz, -OCH₂CH₃), 3.49 (2H, q, *J* = 6.9 Hz, -OCH₂CH₃), 3.58 and 3.70 (each 2H, m, -OCH₂CH₂O-), 4.70 (2H, m, 1,2,3-triazole-CH₂O-), 4.82 (1H, d, *J* = 5.9 Hz, HO-3), 5.22 (1H, d, *J* = 5.9 Hz, H-3), 7.20 (1H, s, H-1), 7.70 and 8.01 (each 2H, m, 1-phenyl), 8.04, 8.56, and 8.88 (each 1H, s, 1,2,4-triazole and 1,2,3-triazole); UV λ_{max} (MeOH) nm (ε): 269.8 (21,000); HRMS (ESI-TOF, positive mode): calcd for C₂₂H₃₀N₆O₃Na [M+Na]⁺ 449.2277, found 449.2276.

4.2.2. (*E*)-1-(4-(4-((2-(2-propoxyethoxy)ethoxy)methyl)-1*H*-1,2,3-triazol-1-yl)phenyl)-4,4-dimethyl-2-(1*H*-1,2,4-triazol-1-yl)pent-1-en-3-ol (Abz-E2P)

To a stirred solution of 1-propanol (2 mL) was added NaH (60% in oil, 77 mg, 1.9 mmol) at room temperature under Ar. After stirred for 15 min, Abz-E1 (100 mg, 168 μmol) dissolved in 1-propanol (3 mL) was added. The mixture was stirred for 18 h at room temperature. After quenched with sat. NH₄Cl, the resulting mixture was extracted with EtOAc (15 mL × 3). The organic layer was washed with brine, dried over Na₂SO₄, and concentrated in vacuo. The residual oil was purified by silica gel column chromatography with 3% MeOH in CH₂Cl₂ to obtain **Abz-E2P** (71.2 mg, 77%) as a pale yellow oil. ¹H NMR (270 MHz, CDCl₃): δ 0.68 (9H, s, *t*-butyl), 0.90 (3H, t, *J* = 7.3 Hz, -OCH₂CH₂CH₃), 1.60 (2H, qt, *J* = 7.3 and 6.9 Hz, -OCH₂CH₂CH₃), 3.42 (2H, t, *J* = 6.9 Hz, -OCH₂CH₂CH₃), 3.59-3.79 (8H, m,

-OCH₂CH₂OCH₂CH₂O-), 4.37 (1H, d, *J* = 8.6 Hz, *HO*-3), 4.60 (1H, d, *J* = 8.6 Hz, H-3), 4.81 (2H, s, 1,2,3-triazole-CH₂O-), 7.00 (1H, s, H-1), 7.56 (2H, m, 1-phenyl), 7.82 (2H, m, 1-phenyl), 8.07 (2H, m, 1,2,4-triazole and 1,2,3-triazole), 8.54 (1H, s, 1,2,4-triazole); UV λ_{max} (MeOH) nm (ε): 269.8 (22,000); HRMS (ESI-TOF, positive mode): calcd for C₂₅H₃₆N₆O₄Na [M+Na]⁺ 507.2696, found 507.2698.

4.2.3. (*E*)-1-(4-(4-((2-(2-butoxyethoxy)ethoxy)methyl)-1*H*-1,2,3-triazol-1-yl)phenyl)-4,4-dimethyl-2-(1*H*-1,2,4-triazol-1-yl)pent-1-en-3-ol (Abz-E2B)

To a stirred solution of 1-butanol (2 mL) was added NaH (60% in oil, 86 mg, 2.1 mmol) at room temperature under Ar. After stirred for 15 min, Abz-E1 (100 mg, 168 μmol) dissolved in 1-propanol (3 mL) was added. The mixture was stirred for 19 h at room temperature. After quenched with sat. NH₄Cl, the resulting mixture was extracted with EtOAc (15 mL × 3). The organic layer was washed with brine, dried over Na₂SO₄, and concentrated in vacuo. The residual oil was purified by silica gel column chromatography with 3% MeOH in CH₂Cl₂ to obtain (±)-Abz-E2B (71.4 mg, 85%), which was further purified for bioassays by HPLC (YMC Hydrosphere C18, 150 × 20 mm, 55% MeOH, 9.0 ml min⁻¹, 254 nm) to obtain a colorless oil (70.5 mg). ¹H NMR (270 MHz, CDCl₃): δ 0.68 (9H, s, *t*-butyl), 0.90 (3H, t, *J* = 7.3 Hz, -O CH₂CH₂CH₂CH₃), 1.35 (2H, m, -OCH₂CH₂CH₂CH₃), 1.56 (2H, m, -OCH₂CH₂CH₂CH₃), 3.46 (2H, t, *J* = 6.6 Hz, -OCH₂CH₂CH₂CH₃), 3.60-3.78 (8H, m, -OCH₂CH₂OCH₂CH₂O-), 4.35 (1H, d, *J* = 8.9 Hz, *HO*-3), 4.60 (1H, d, *J* = 8.9 Hz, H-3), 4.80 (2H, s, 1,2,3-triazole-CH₂O-), 7.00 (1H, s, H-1), 7.56 (2H, m, 1-phenyl), 7.82 (2H, m, 1-phenyl), 8.08 (2H, m, 1,2,4-triazole and 1,2,3-triazole), 8.54 (1H, s, 1,2,4-triazole); UV λ_{max} (MeOH) nm (ε): 269.2 (21,000); HRMS (ESI-TOF, positive mode): calcd for C₂₆H₃₈N₆O₄Na [M+Na]⁺ 521.2852, found 521.2855.

4.3. Determination of the absolute configuration of optically pure Abz-E2B by advanced Mosher's method

4.3.1. Optical resolution of Abz-E1

(±)-Abz-E1 (27 mg) was subjected to chiral HPLC under the following conditions: column, Chiralpak AD-H (250 × 10 mm, Daicel); solvent, 35% EtOH in hexane; flow rate, 5 mL min⁻¹; detection, 254 nm. The materials at t_R 29.5-32.5 and 36.7-40.5 min were collected to give (+)-Abz-E1 (12.9 mg) and (-)-Abz-E1 (13.6 mg), respectively, with an optical purity of each 99.9%. (+)-Abz-E1: $[\alpha]_D^{23} +18.6$ (MeOH, c 0.860); (-)-Abz-E1: $[\alpha]_D^{23} -23.7$ (MeOH, c 0.907). ¹H NMR and HRMS data of optically pure Abz-E1 agreed with those of racemic Abz-E1.

4.3.2. Preparation of optically pure Abz-E2B

(+)-Abz-E2B (3.6 mg) and (-)-Abz-E2B (5.1 mg) were prepared from (+)-Abz-E1 (10 mg) respectively in the same manner as (±)-Abz-E2B. (+)-Abz-E2B: ¹H NMR (270 MHz, CDCl₃): δ 0.68 (9H, s, *t*-butyl), 0.90 (3H, t, $J = 7.5$ Hz, -OCH₂CH₂CH₂CH₃), 1.36 (2H, m, -OCH₂CH₂CH₂CH₃), 1.56 (2H, m, -OCH₂CH₂CH₂CH₃), 3.46 (2H, t, $J = 6.6$ Hz, -OCH₂CH₂CH₂CH₃), 3.61-3.77 (8H, m, -OCH₂CH₂OCH₂CH₂O-), 4.35 (1H, d, $J = 8.9$ Hz, HO-3), 4.60 (1H, d, $J = 8.9$ Hz, H-3), 4.80 (2H, s, 1,2,3-triazole-CH₂O-), 7.00 (1H, s, H-1), 7.56 (2H, m, 1-phenyl), 7.82 (2H, m, 1-phenyl), 8.07 (1H, s, 1,2,4-triazole), 8.08 (1H, s, 1,2,3-triazole), 8.54 (1H, s, 1,2,4-triazole); ¹³C NMR (67.8 MHz, CDCl₃): δ 13.9 (-OCH₂CH₂CH₂CH₃), 19.3 (-OCH₂CH₂CH₂CH₃), 26.1 (methyls in *t*-butyl), 31.7 (-OCH₂CH₂CH₂CH₃), 36.3 (tertiary carbon in *t*-butyl), 64.7, 70.0, 70.1, 70.6, and 70.7 (diethylene glycol linker), 71.2 (-OCH₂CH₂CH₂CH₃), 75.8 (C3), 120.6 (1,2,3-triazole), 120.7 (phenyl), 127.5 (C1), 130.3 (phenyl), 134.3 (phenyl), 136.7 (phenyl), 137.8 (C2), 143.2 (1,2,4-triazole), 146.4 (1,2,3-triazole), 151.7 (1,2,4-triazole); HRMS (ESI-TOF, positive mode): calcd for C₂₆H₃₈N₆O₄Na [M+Na]⁺ 521.2852, found 521.2843; $[\alpha]_D^{26} +24.7$ (MeOH, c 0.146). (-)-Abz-E2B: ¹H NMR (270 MHz, CDCl₃): δ 0.68 (9H, s, *t*-butyl), 0.90 (3H, t, $J = 7.3$ Hz, -OCH₂CH₂CH₂CH₃), 1.34 (2H, m, -OCH₂CH₂CH₂CH₃), 1.56 (2H, m, -OCH₂CH₂CH₂CH₃), 3.46 (2H, t, $J = 6.6$ Hz, -OCH₂CH₂CH₂CH₃), 3.60-3.76 (8H, m, -OCH₂CH₂OCH₂CH₂O-), 4.35 (1H, d, $J = 8.9$ Hz, HO-3), 4.60 (1H, d, $J = 8.9$ Hz, H-3), 4.80

(2H, s, 1,2,3-triazole-CH₂O-), 7.00 (1H, s, H-1), 7.56 (2H, m, 1-phenyl), 7.82 (2H, m, 1-phenyl), 8.07 (2H, s, 1,2,4-triazole and 1,2,3-triazole, overlapped), 8.54 (1H, s, 1,2,4-triazole); ¹³C NMR (67.8 MHz, CDCl₃): δ 13.9 (-OCH₂CH₂CH₂CH₃), 19.3 (-OCH₂CH₂CH₂CH₃), 26.1 (methyls in *t*-butyl), 31.7 (-OCH₂CH₂CH₂CH₃), 36.3 (tertiary carbon in *t*-butyl), 64.7, 70.0, 70.1, 70.6, and 70.7 (diethylene glycol linker), 71.2 (-OCH₂CH₂CH₂CH₃), 75.8 (C3), 120.6 (1,2,3-triazole), 120.7 (phenyl), 127.5 (C1), 130.3 (phenyl), 134.3 (phenyl), 136.7 (phenyl), 137.7 (C2), 143.2 (1,2,4-triazole), 146.4 (1,2,3-triazole), 151.7 (1,2,4-triazole); HRMS (ESI-TOF, positive mode): calcd for C₂₆H₃₈N₆O₄Na [M+Na]⁺ 521.2852, found 521.2857; (+)-Abz-E2B: [α]_D²⁷ -24.1 (MeOH, *c* 0.157). Protons of 1,2,4-triazole and 1,2,3-triazole were assigned on the basis of an HMBC correlation: -N-CH=C(N=N-)-CH₂O-.

4.3.3. Preparation of *R*-MTPA-esters of the optically pure Abz-E2B

To a stirred solution of (±)-Abz-E2B (50 mg, 100 μmol) in dry pyridine-CH₂Cl₂ (1:1, 450 μl) was added dimethylaminopyridine (78.9 mg, 703 μmol) and *S*-α-methoxy-α-(trifluoromethyl)phenylacetyl chloride (MTPA-Cl) (55 μl, 293 μmol). After stirred for 6 h, water was added to quench the reaction. The resulting mixture was extracted with EtOAc (7 mL × 3). The organic layer was washed with brine, dried over Na₂SO₄, and concentrated in vacuo. The residual oil was purified by silica gel column chromatography with 70% EtOAc in hexane to obtain *R*-MTPA-(±)-Abz-E2B (55 mg, 63 μmol, 63%) as a pale yellow oil. *R*-MTPA-(±)-Abz-E2B (55 mg) was diastereomerically resolved by silicagel HPLC (YMC-Pack SIL-06, 150 × 20 mm, 30% 2-propanol in hexane, 4.0 ml min⁻¹, 254 nm) and subsequently purified by chiral HPLC (Chiralpak AD-H, 250 × 10 mm, Daicel; solvent, 20% EtOH in hexane; flow rate, 4 mL min⁻¹; detection, 254 nm) to obtain the diastereomer A (***R*-MTPA(-)-Abz-E2B**, 15.6 mg) and the diastereomer B (***R*-MTPA(+)-Abz-E2B**, 5.6 mg). Although the sign of the rotation of Abz-E2B in each diastereomer was specified in parentheses to avoid confusion, it was yet unknown at this time and determined by identifying the rotational sign of Abz-E2B released from the MTPA esters (see 4.3.4). ¹H NMR (500 MHz,

CDCl₃): diastereomer A (**R-MTPA-(+)-Abz-E2B**): δ 0.74 (9H, s, *t*-butyl), 0.90 (3H, t, $J = 7.3$ Hz, -O CH₂CH₂CH₂CH₃), 1.35 (2H, m, -OCH₂CH₂CH₂CH₃), 1.56 (2H, m, -OCH₂CH₂CH₂CH₃), 3.47 (2H, t, $J = 6.6$ Hz, -OCH₂CH₂CH₂CH₃), 3.60-3.77 (11H, m, 4 × -CH₂O- and -OMe), 4.81 (2H, s, 1,2,3-triazole-CH₂O-), 6.15 (1H, s, H-3), 7.26 (1H, s, H-1), 7.44 (3H, m, phenyl in MTPA), 7.60 (2H, m, phenyl in MTPA), 7.67 and 7.87 (each 2H, m, 1-phenyl), 7.82 and 7.94 (each 1H, s, 1,2,4-triazole), 8.09 (1H, s, 1,2,3-triazole); diastereomer B (**R-MTPA-(-)-Abz-E2B**): δ 0.67 (9H, s, *t*-butyl), 0.90 (3H, t, $J = 7.3$ Hz, -O CH₂CH₂CH₂CH₃), 1.36 (2H, m, -OCH₂CH₂CH₂CH₃), 1.56 (2H, m, -OCH₂CH₂CH₂CH₃), 3.47 (2H, t, $J = 6.6$ Hz, -OCH₂CH₂CH₂CH₃), 3.51 (3H, s, -OMe), 3.60-3.77 (11H, m, 4 × -CH₂O-), 4.81 (2H, s, 1,2,3-triazole-CH₂O-), 6.21 (1H, s, H-3), 7.35 (1H, s, H-1), 7.48 (3H, m, phenyl in MTPA), 7.60 (2H, m, phenyl in MTPA), 7.68 and 7.86 (each 2H, m, 1-phenyl), 7.80 and 8.08 (each 1H, s, 1,2,4-triazole), 8.09 (1H, s, 1,2,3-triazole). Protons of 1,2,4-triazole and 1,2,3-triazole were assigned on the basis of an HMBC correlation: -N-CH=C(N=N-)-CH₂O-.

4.3.4. Hydrolysis of the diastereomers A and B

To a stirred solution of the diastereomer A (5.6 mg, 7.8 μ mol) in MeOH (1.2 mL) was added 1 M NaOH (1 mL). After stirred for 1.5 h, 1 M HCl (1.5 mL) was added to quench the reaction. The resulting mixture was extracted with EtOAc (8 mL × 3). The organic layer was washed with brine, dried over Na₂SO₄, and concentrated in vacuo. The residual oil was purified by silica gel column chromatography with 5% MeOH in CH₂Cl₂ to obtain a crude oil containing Abz-E2B. The crude oil was further purified by HPLC (YMC Hydrosphere C18, 150 × 20 mm, 70% MeOH, 8.0 ml min⁻¹, 254 nm) to obtain Abz-E2B (2.8 mg, 5.6 μ mol, 72%) as a colorless oil. In the same manner as the diastereomer A, the diastereomer B (15.6 mg, 21.8 μ mol) was hydrolyzed to release Abz-E2B (4.5 mg, 9.0 μ mol, 41%) as a colorless oil. Abz-E2B obtained from the diastereomers A and B were determined to be the (+)- and (-)-isomers, respectively, on the basis of chiral HPLC analysis (see 4.3.2).

4.4. Water-solubility test

MeOH solutions of test samples were put in a glass vial and concentrated in vacuo. Distilled water (2 mL) or MeOH (2 mL) was added to the vial. After shaking several times and leaving to stand for 1 h, 5 μL of the solution was subjected to HPLC. HPLC conditions were: ODS column, Hydrosphere C18 (150 \times 6.0 mm, YMC); solvent, 85% MeOH in H_2O ; flow rate, 1.0 mL min^{-1} ; detection, 254 nm. Solubility (%) in water was calculated based on the in water/in MeOH ratio of the HPLC peak area.

4.5. Preparation of recombinant enzymes

4.5.1. Coexpression of recombinant *Arabidopsis* CYP707A3 and *Arabidopsis* P450 reductase (ATR2) in *E. coli*

A truncated *Arabidopsis* CYP707A3 (707A3d28), which lacked the putative membrane-spanning segment of the N-terminus, residues 3-28, was constructed. Cells of *E. coli* strain BL21 were transformed with the constructs pCW-CYP707A3d28 and pACYC-AR2. Cultures (3 mL) were grown overnight in Luria-Bertani medium supplemented with ampicillin (50 $\mu\text{g mL}^{-1}$) and chloramphenicol (100 $\mu\text{g mL}^{-1}$). Then, 50 mL of Terrific Broth medium supplemented with ampicillin (50 $\mu\text{g mL}^{-1}$), chloramphenicol (100 $\mu\text{g mL}^{-1}$), and aminolevulinic acid (0.5 mM) was inoculated with an aliquot of the overnight culture (0.5 mL). The culture was incubated with gentle shaking (225 rpm) at 37 $^{\circ}\text{C}$ until A_{600} reached 0.6 (at 2.5–3 h), and expression of the P450 enzyme was induced by the addition of isopropyl β -D-thiogalactopyranoside (0.1 mM). The culture was shaken continuously (150 rpm) at 25 $^{\circ}\text{C}$ and cells were harvested 48 h later by centrifugation at 2,330 $\times g$ for 20 min at 4 $^{\circ}\text{C}$. Pelleted cells were suspended in 2.5 mL of buffer A (50 mM potassium phosphate buffer, pH 7.25, 20% glycerol, 1 mM EDTA, 0.1 mM dithiothreitol). The suspension was sonicated for 30 s, and the enzyme solution in the supernatant was collected by centrifugation at 23,470 $\times g$ for 30 min at 4 $^{\circ}\text{C}$. The P450 content was determined by spectrophotometric analysis, using the extinction coefficient of a reduced CO difference spectrum (91.1 $\text{mM}^{-1} \text{cm}^{-1}$).

4.5.2. Cloning and heterologous expression of OsCYP701A6 with a baculovirus-insect cell system

cDNA containing the entire open-reading frame of OsCYP701A6 was amplified by RT-PCR. The full-length OsCYP701A6 (AK066285) was obtained from the Rice Genome Resource Center (the National Institute of Agrobiological Sciences, Japan), and the OsCYP701A6 ORF was amplified by PCR with the full-length cDNA as template. Nucleotide sequences of gene-specific primers were as follows: TO-35: 5'-AAAACTAGTATGGAGGCGTTCGTGC-3' (*SpeI* site in italics and start codon underlined) and TO-36: 5'-AAAATTCGAATCACATCCTTCCTCTGCG-3' (*HindIII* site in italics and stop codon underlined). A 1-ng aliquot of the full-length cDNA was used as a template for the PCR reaction in a 20- μ L reaction mixture containing 5 x PrimeSTAR Buffer (Mg^{2+} plus) (4 μ L), PrimeSTAR HS DNA Polymerase (0.5 U), 200 μ M dNTP mixture, and 0.2 μ M of the gene-specific primers described above. The PCR product was gel-purified and cloned into pJET1.2/blunt using a CloneJET PCR Cloning Kit (Fermentas, Canada). The cloned inserts were sequenced with pJET1.2 forward and reverse sequencing primers to confirm the absence of PCR errors in the inserts. Full-length cDNA of OsCYP701A6 in pJET1.2/blunt plasmid vector was excised with the restriction enzymes *SpeI* and *HindIII* (TaKaRa Bio) and purified by 1% (w/v) agarose gel electrophoresis. This cDNA was ligated into pFastBac1 vector (Invitrogen, USA) digested with the same set of restriction enzymes. The pFastBac1-OsCYP701A6 constructs were used for the preparation of recombinant bacmid DNA by transformation of *E. coli* strain DH10Bac (Invitrogen). Preparation of recombinant baculovirus DNA containing OsCYP701A6 cDNA and transfection of *Sf9* (*Spodoptera frugiperda* 9) cells were performed according to the manufacturer's protocol (Invitrogen). For expression of OsCYP701A6, *Sf9* cells infected by baculovirus containing OsCYP701A6 cDNA were incubated in Grace's insect cell medium, 0.1% (w/v) Pluronic F-68 (Invitrogen), 10% (v/v) fetal bovine serum, 100 μ M 5-aminolevulinic acid and 100 μ M ferrous citrate on a rotary shaker at 27 °C and 150 rpm for 96 h. Insect cells were then harvested by

centrifugation at 3,000 x g for 10 min and washed with PBS buffer three times. After centrifuging again, insect cells were sonicated in buffer A containing 50 mM potassium phosphate (pH 7.3), 20% (v/v) glycerol, 1 mM EDTA, 0.1 mM dithiothreitol and centrifuged at 8,000 x g for 10 min. The supernatant was further centrifuged at 100,000 x g for 1 h and the resulting pellet (microsomal fraction) was homogenized with buffer A. The concentration of active P450 was estimated from the carbon monoxide difference spectrum.²⁹

4.6. Enzyme assay

4.6.1. CYP707A3

A reaction mixture containing 25 $\mu\text{g mL}^{-1}$ of CYP707A3 microsomes coexpressed AR2 in *E. coli*, (+)-ABA (final conc. 1–64 μM), inhibitors (0 for control, 5–10000 nM in 5 μL DMF) and 130 μM NADPH in 100 mM potassium phosphate buffer (pH 7.25) were incubated for 10 min at 30 °C. Reactions were initiated by adding NADPH, and stopped by addition of 50 μL of 1 M NaOH. Each reaction mixture was acidified with 100 μL of 1 M HCl. To extract the reaction products, the mixture was loaded onto an Oasis HLB cartridge (1 mL, 30 mg; Waters) and washed with 1 mL of 10% MeOH in H₂O containing 1% AcOH. The enzyme products were then eluted with 1 mL of MeOH containing 1% AcOH, and the eluate was concentrated in vacuo. The dried sample was dissolved in 50 μL of MeOH, and 20 μL was subjected to HPLC. HPLC conditions were: ODS column, Hydrosphere C18 (150 × 6.0 mm, YMC); solvent, 20% MeCN in H₂O containing 0.1% AcOH; flow rate, 1.0 mL min⁻¹; detection, 254 nm. Enzyme activity was confirmed by determining the amount of PA in control experiments before each set of measurements. Inhibition constants were determined using the Enzyme Kinetics module of SigmaPlot 10 software³⁰ after determining the mode of inhibition by plotting the reaction velocity in the presence and absence of inhibitor on a double-reciprocal plot. All assays were conducted at least twice.

4.6.2. CYP701A6

The microsomal fractions of OsCYP701A6 were combined with purified NADPH-P450 reductase.³¹ A reaction mixture containing OsCYP701A6 microsomal fraction (25 pmol), ATR2 (0.125 U), *ent*-kaurene (10 μ M, final conc. after addition of NADPH) as substrate, and inhibitor (0.03-10 μ M, final conc. after addition of NADPH) in 50 mM potassium phosphate buffer (pH 7.25, 380 μ L) was preincubated at 30 °C for 5 min. Reactions were initiated by addition of 20 mM NADPH (20 μ L), and were carried out at 30 °C for 30 min. After termination by adding 1 M HCl (100 μ L) and EtOAc (200 μ L), 5 μ L of 1 mM abietic acid was added as an internal standard. The reaction products were extracted three times with an equal volume of ethyl acetate and the organic phase was collected. Anhydrous Na₂SO₄ was added to remove residual water. To derivatize the reaction products, methanol (100 μ L) and TMS-CHN₂ (100 μ L) (2.0 M in Et₂O) were added and the reaction mixture was incubated at room temperature for 15 min. Organic solvent was removed under Ar and samples were adjusted to 200 μ L with Et₂O before GC-MS analysis (QP2010-plus, Shimadzu Corp., Japan). GC conditions were: column, DB-5ms (0.25 mm i.d. \times 15 m; 0.25 μ m film thickness; J&W Scientific); carrier gas, He; flow rate, 1.84 ml min⁻¹; injection port temperature, 280 °C; splitless injection; column oven temperature, 80 °C (1 min), 80-200 °C (18 °C min⁻¹), 200-210 °C (2 °C min⁻¹), 210-280 °C (30 °C min⁻¹), 280 °C (3 min). The content of KA was calculated from the area ratio of molecular and fragment ions of methyl KA (*m/z* 316, 273, and 257) to those of methyl abietate (*m/z* 316 and 256).

4.7. Bioassays

4.7.1. Arabidopsis seed germination assay

Twenty-five seeds (Col-0) were sterilized successively with 70% (v/v) EtOH for 30 min and reagent grade EtOH for 1 min. The sterilized seeds were soaked in 250 μ L of a test solution and incubated in the dark for 3 days at 5 °C. The vernalized seeds in the test solution were transferred to 24-well plates placed on two sheets of filter paper, and allowed to germinate under continuous light for 24 h at 22 °C. All assays were conducted at least twice.

4.7.2. Lettuce seed germination and growth assays

Five seeds (*Lactuca sativa* L. cv. Grand Rapids) were placed in 24-well plates on two sheets of filter paper soaked in 0.2 mL of a test solution and allowed to germinate and grow under continuous light for 23 days at 22 °C. All assays were conducted at least twice.

4.7.3. Rice seedling elongation assay

Seeds of rice (*O. sativa* L. cv. Nipponbare) were sterilized with EtOH for 5 min and washed with running tap water. The sterilized seeds were soaked in water for 3 days at 25 °C to germinate. The seeds were then placed in a glass tube containing 2 mL of a test solution and grown with the tube sealed with a plastic cap under continuous light at 25 °C. When the seedlings were 7 days old, the length of the second leaf sheath was measured. All assays were conducted at least twice.

4.7.4. Bent grasses drought tolerance assay

Bent grass (*Agrostis capillaris*), which was planted in a plastic box with moist vermiculite and grown in a greenhouse covered with polyvinyl film, was used in these experiments. A 0.2% (v/v) Hyponex nutrient solution (Hyponex Japan Co., Ltd, Osaka, Japan) was supplied at 2 L m⁻² to vermiculite at 14 day intervals. The temperature ranged from 25 to 33 °C during the day (6 a.m. to 6 p.m.) and 23 to 25 °C at night (6 p.m. to 6 a.m.). The relative humidity (RH) was 45-65% during the day and 65-75% at night. Ninety-day-old bent grass was planted uniformly in a plastic box 40 cm wide, 40 cm long and 5 cm deep, watered, then sprayed with a test solution (50 μM Abz-E2B) or distilled water. The boxes were then put in a controlled room at 350 μmol m⁻² s⁻¹ photosynthetic photon flux at 25 °C and 60% RH. The bent grass was grown for 10 days under dehydration conditions (water not supplied to the vermiculite) until rehydration (a sufficient amount of water was supplied to the vermiculite). Under dehydration and rehydration conditions, leaves of bent grass were sampled for analysis of endogenous ABA content. The extraction and quantification of ABA in apple seedlings were performed according to a method similar to that reported previously in apple seedlings³² using

HPLC and gas chromatography-mass spectrometry-selective ion monitoring (GC-MS-SIM) (Shimadzu QP5000). ABA was calculated by the ratio of peak areas for m/z 190(d_0)/194(d_6). 3',5',5',7',7',7'-Hexadeuterated ABA (ABA- d_6) was purchased from Shoko Co. (Tokyo, Japan).

Acknowledgments

We thank Prof. Akira Kitajima (Kyoto University) for kindly providing rice (Nipponbare) seeds. We thank Toray Industries Inc., Tokyo, Japan, for a gift of (+)-ABA. Part of this research was carried out using an instrument at the Center for Instrumental Analysis of Shizuoka University. This research was supported by a Grant-in-Aid for Scientific Research (No. 22580118) from the Ministry of Education, Culture, Sports, Science and Technology of Japan.

Supplementary data

Supplementary data associated with this article can be found in the online version at doi:xx.xxxx/j.bmc.201x.xx.xxx.

References and notes

1. Hirai, N. Abscisic acid. In *Comprehensive Natural Products Chemistry* Vol. 8; Mori, K. Ed.; Elsevier: Amsterdam, 1999; pp 72-91.
2. Davies, W. J.; Jones, H. G. *Abscisic Acid*; BIOS Scientific Publishers: Oxford, 1991.
3. Zeevaart, J. A. D.; Creelman, R. A. *Annu. Rev. Plant Physiol. Plant Mol. Biol.* **1998**, *39*, 439.
4. Nambara, E.; Marion-Poll, A. *Annu. Rev. Plant Biol.* **2005**, *56*, 165.
5. Huang, D.; Jaradat, MR.; Wu, W.; Ambrose, S. J.; Ross, A. R.; Abrams, S. R.; Cutler, A.

J. Plant J. **2007**, *50*, 414.

6. Loveys, B. R. In *Abscisic Acid*; Davies, W. J.; Jones, H. G. Eds; BIOS Scientific Publishers: Oxford, 1991.
7. Saito, S.; Hirai, N.; Matsumoto, C.; Ohigashi, H.; Ohta, D.; Sakata, K.; Mizutani, M. *Plant Physiol.* **2004**, *134*, 1439.
8. Kushiro, T.; Okamoto, M.; Nakabayashi, K.; Yamagishi, K.; Kitamura, S.; Asami, T.; Hirai, N.; Koshiba, T.; Kamiya, Y.; Nambara, E. *ENBO J.* **2004**, *23*, 1647.
9. Yang, S. H.; Choi, D. *Biochem. Biophys. Res. Commun.* **2006**, *350*, 685.
10. Yang, S. H.; Zeevaart, J. A. D. *Plant J.* **2006**, *47*, 675.
11. Millar, A. A.; Jacobsen, J. V.; Ross, J. J.; Helliwell, C. A.; Poole, A. T.; Scofield, G.; Reid, J. B.; Gubler, F. *Plant J.* **2006**, *45*, 942.
12. Destefano-Beltran, L.; Knauber, D.; Huckle, L.; Suttle, J. C. *Plant Mol Biol.* **2006**, *61*, 687.
13. Umezawa, T.; Okamoto, M.; Kushiro, T.; Nambara, E.; Oono, Y.; Seki, M.; Kobayashi, M.; Koshiba, T.; Kamiya, Y.; Shinozaki, K. *Plant J.* **2006**, *46*, 171.
14. Okamoto, M.; Kuwahara, A.; Seo, M.; Kushiro, T.; Asami, T.; Hirai, N.; Kamiya, Y.; Koshiba, T.; Nambara, E. *Plant Physiol.* **2006**, *141*, 97.
15. Funaki, Y.; Ishiguri, T.; Kato, T.; Tanaka, S. *J. Pesticide Sci.* **1984**, *9*, 229.
16. Funaki, Y.; Oshita, H.; Yamamoto, S.; Tanaka, S.; Kato, T. (Sumitomo Chemical Co.). Ger. Offen. DE3010560, 1980.
17. Saito, S.; Okamoto, M.; Shinoda, S.; Kushiro, T.; Koshiba, T.; Kamiya, Y.; Hirai, N.; Todoroki, Y.; Sakata, K.; Nambara, E.; Mizutani, M. *Biosci. Biotechnol. Biochem.* **2006**, *70*, 1731.
18. Izumi, K.; Kamiya, Y.; Sakurai, A.; Oshio, H.; Takahashi, N. *Plant Cell Physiol.* **1985**, *26*, 821.
19. Kitahata, N.; Saito, S.; Miyazawa, Y.; Umezawa, T.; Shimada, Y.; Min, Y. K.; Mizutani, M.; Hirai, N.; Shinozaki, K.; Yoshida, S.; Asami, T. *Bioorg. Med. Chem.* **2005**, *13*, 4491.
20. Fletcher, R. A.; Hofstra, G.; Gao, J.-G. *Plant Cell Physiol.* **1986**, *27*, 367.

21. Todoroki, Y.; Ueno, K. *Cur. Med. Chem.* **2010**, *17*, 3230.
22. Todoroki, Y.; Aoyama, H.; Hiramatsu, S.; Shirakura, M.; Nimitkeatkai, H.; Kondo, S.; Ueno, K.; Mizutani, M.; Hirai, N. *Bioorg. Med. Chem. Lett.* **2009**, *19*, 5782.
23. Todoroki, Y.; Kobayashi, K.; Shirakura, M.; Aoyama, H.; Takatori, K.; Nimitkeatkai, H.; Jin, M.-H.; Hiramatsu, S.; Ueno, K.; Kondo, S.; Mizutani, M.; Hirai, N. *Bioorg. Med. Chem.* **2009**, *17*, 6620.
24. Todoroki, Y.; Naiki, K.; Aoyama, H.; Shirakura, M.; Ueno, K.; Mizutani, M.; Hirai, N. *Bioorg. Med. Chem. Lett.* **2010**, *20*, 5506.
25. Okazaki, M.; Nimitkeatkai, H.; Muramatsu, T.; Aoyama, H.; Ueno, K.; Mizutani, M.; Hirai, N.; Kondo, S.; Ohnishi, T.; Todoroki, Y. *Bioorg. Med. Chem.* **2011**, *19*, 406.
26. Ohtani, I.; Kusumi, T.; Kashman, Y.; Kakisawa, H. *J. Am. Chem. Soc.* **1991**, *113*, 4092.
27. Todoroki, Y.; Kobayashi, K.; Yoneyama, H.; Hiramatsu, S.; Jin, M.-H.; Watanabe, B.; Mizutani, M.; Hirai, N. *Bioorg. Med. Chem.* **2008**, *16*, 3141.
28. Ueno, K.; Yoneyama, H.; Mizutani, M.; Hirai, N.; Todoroki, Y. *Bioorg. Med. Chem.* **2007**, *15*, 6311.
29. Omura, T.; Sato, R. *J. Biol. Chem.* **1964**, *239*, 2370.
30. *SigmaPlot 10*; Systat Software, Inc.: Richmond CA, 2006.
31. Mizutani, M.; Ohta, D. *Plant Physiol.* **1998**, *116*, 357.
32. Kondo, S.; Ponrod, W.; Kanlayanarat, S.; Hirai, N. *J. Am. Soc. Hort. Sci.* **2002**, *127*, 737.

Table 1

Enzymatic, biological, and physicochemical properties of azole inhibitors of CYP707A

Figure 1. Specific inhibitors of ABA 8'-hydroxylase (CYP707A). These were developed from *S*-UNI, which is a potent inhibitor of both CYP707A and *ent*-kaurene oxidase (CYP701A). A disadvantage of *UTn* is its poor water solubility.²² *Abz-E1* has improved water solubility but it is potentially unstable owing to the tosylate group.²⁵ This work describes the development of *Abz-E2P* and *Abz-E2B* as novel CYP707A inhibitors that are chemically stable and more water soluble.

Figure 2. Comparison of effect of (\pm)-*Abz-E2P*, (\pm)-*Abz-E2B* and *S*-UNI on rice seedling growth on day 7 after treatment. *S*-UNI was not tested at a concentration greater than 30 μ M in this experiment. Images of seedlings treated with (\pm)-*Abz-E1*, which were obtained in earlier work,²⁵ are shown for comparison.

Figure 3. Enhancement of (\pm)-*Abz-E2P* and (\pm)-*Abz-E2B* on ABA activity: (a) inhibition of lettuce seed germination at 24 h ($n=2$), (b) inhibition of lettuce seedling growth at 168 h, (c) inhibition of *Arabidopsis* seed germination at 24 h ($n=2$), (d) leaf emergence in *Arabidopsis* at 96 h after imbibition.

Figure 4. Effect of *Abz-E1* (50 μ M) on drought tolerance of bent grass (a) and ABA content of the leaves (b).

Figure 5. Determination of the absolute configuration of optically pure *Abz-E2B* by an advanced Mosher's method. Molecular models of the MTPA esters were optimized with B3LYP/6-31G(d) from the initial geometries with the ideal MTPA plane. Proton signals

of H3" and H5" of 1,2,4-triazole rings were not identified, which is because no HMBC cross-peak was observed between these protons and C2. Stick models: carbons, gray; hydrogens, white; oxygens, red; nitrogens, blue; and fluorines, light green. The structural formulas correspond to views from the right side of the models. The MTPA plane, defined by the trifluoromethyl group, the carbonyl group, and the carbinol proton, are colored in purple in the structural formula.

Figure 6. Enhancement of *R*- and *S*-Abz-E2B on ABA activity: (a) inhibition of lettuce seed germination at 24 h ($n=3$), (b) inhibition of lettuce seedling growth at 216 h, (c) inhibition of *Arabidopsis* seed germination at 24 h ($n=3$), (d) leaf emergence in *Arabidopsis* at 192 h after imbibition.

Figure 7. Comparison of the most stable conformation (A) of *S*- and *R*-UNI and the rotamers of *R*-UNI in the C2-N1" bond (B) and C2-C3 bond (C). Stick models: carbons, gray; hydrogens, white; oxygens, red; nitrogens, blue; and chlorines, green.

Figure 8. Comparison of effect of *R*-Abz-E2B, *S*-Abz-E2B, and *S*-UNI on rice seedling growth on day 7 after treatment (a), and the unstable retardant effect of *S*-Abz-E2B at 100 μ M.

Figure 9. Rescue of rice seedlings on exogenous GA₃ in the presence of *S*-UNI and *S*-Abz-E2B.

Scheme 1. Synthesis of **1** and **2**. Reagents and conditions: LiAlH₄, dry THF, 0 °C→RT, 24% (**1**) and 28% (**2**).

Scheme 2. Synthesis of (±)-Abz-E2P and (±)-Abz-E2B. Reagents and conditions: NaH, propanol or butanol, RT, 77% (Abz-E2P) and 85% (Abz-E2B)

Table 1

Enzymatic, biological, and physicochemical properties of azole inhibitors of CYP707A

Compound	CYP707A inhibition ^a	CYP701A inhibition ^b		Growth inhibition ^c	clog <i>P</i> ^d	Solubility (%) in water (2 mL) ^e	
	<i>K</i> _I (nM)	ratio (%)	IC ₅₀ (μM)	IC ₅₀ (μM)		20 nmol	200 nmol
<i>S</i> -UNI	10	100	0.057	0.18	3.13	79.4	39.5
<i>R</i> -UNI	1450	– ^f	0.300	7.8	3.13	–	–
(±)-UT4	195	–	–	42	3.96	40.7	–
(±)-Abz-E1	27	51	1.0	>100	4.02	68.9	21.3
1	850	0	–	>100	1.46	–	95.7
2	270	3.4	–	>100	2.50	–	99.5
(±)-Abz-E2P	130	20	–	>100	2.98	–	94.8
(±)-Abz-E2B	36	13	–	>100	3.42	–	95.3
<i>S</i> -Abz-E2B	28	–	5.5	>100	3.42	–	–
<i>R</i> -Abz-E2B	360	–	1.1	>100	3.42	–	–

^a *Arabidopsis* recombinant CYP707A3 expressed in *E. coli*.^b Rice recombinant CYP701A6 expressed in insect cells. Inhibition ratios were determined using 0.1 μM test compounds and 10 μM *ent*-kaurene. The inhibition assay for determining the IC₅₀ values was performed using 1 μM *ent*-kaurene.^c Length of the second leaf sheath of rice seedlings.^d Calculated partition coefficient (Marvin, ChemAxon, <http://www.chemaxon.com/marvin/sketch/index.php>).^e Calculated based on the in water to in MeOH ratio of HPLC peak area. The amount of solute: 20 and 200 nmol.^f Not tested.

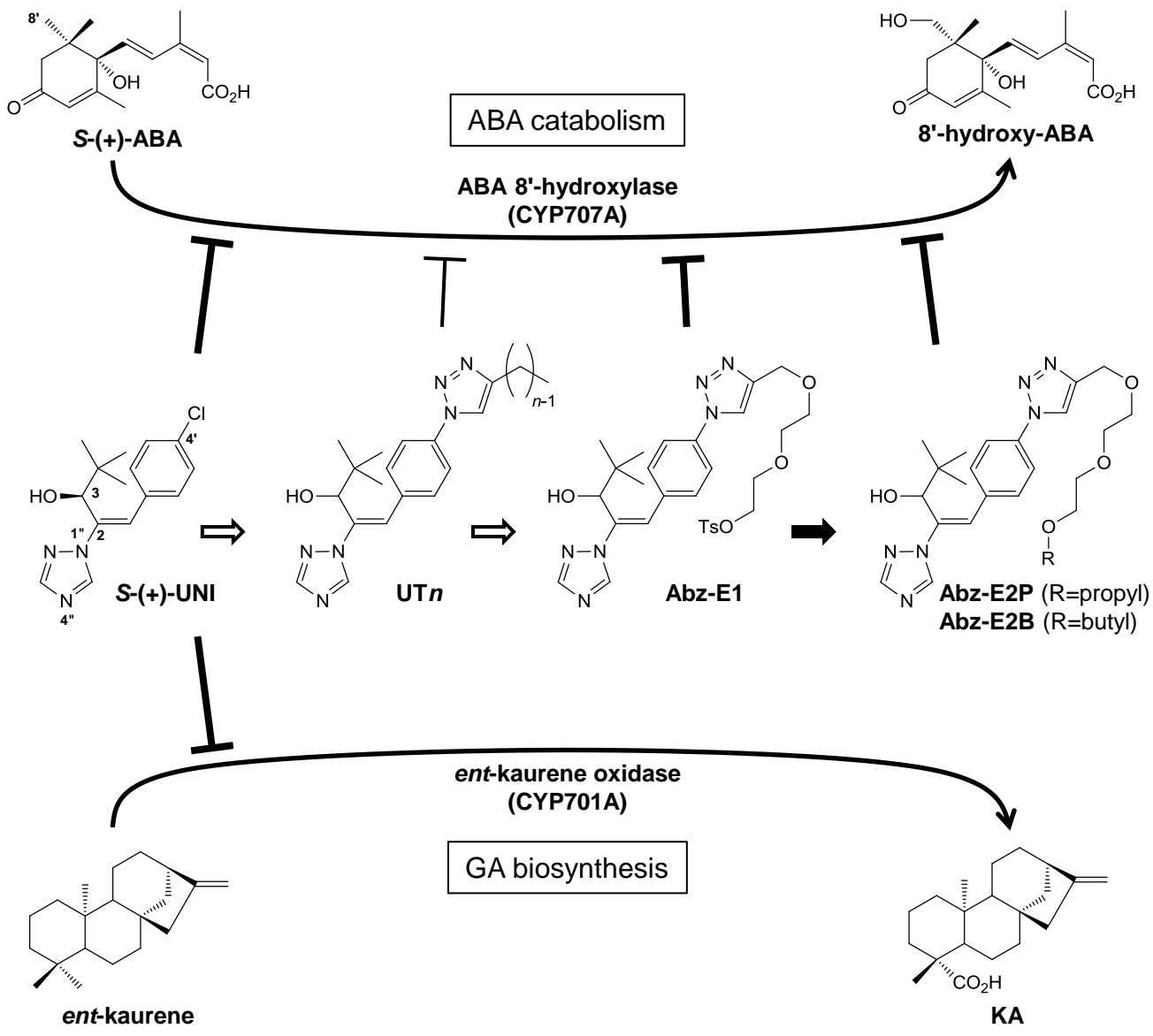


Figure 1

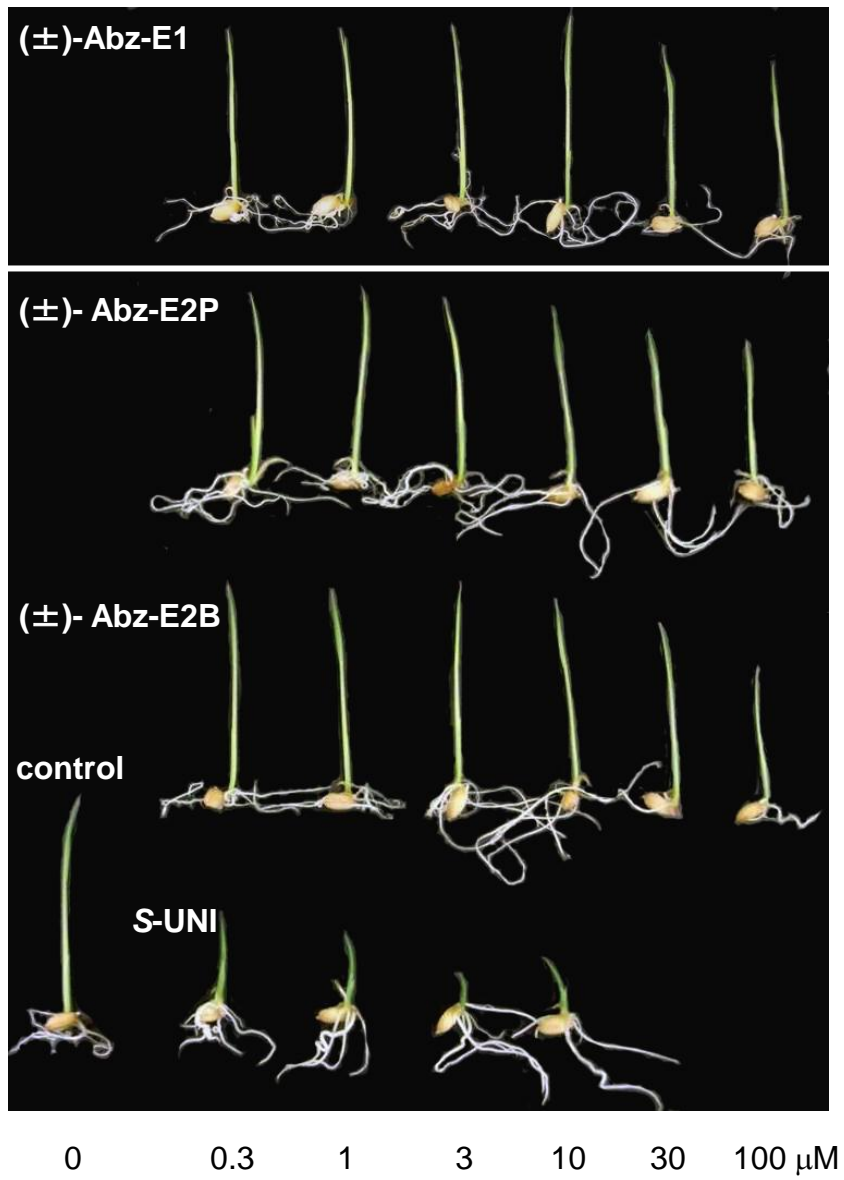


Figure 2

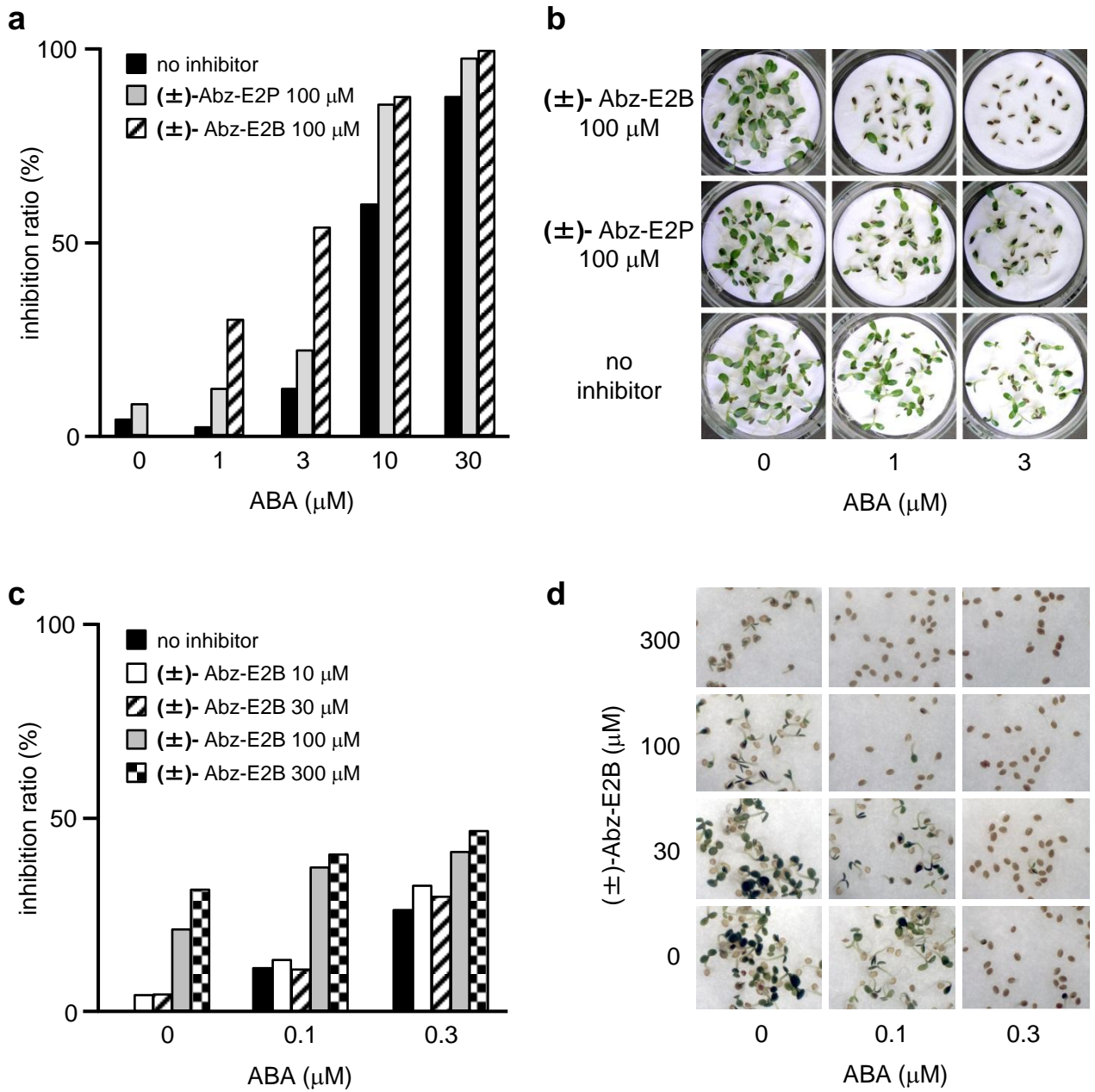


Figure 3

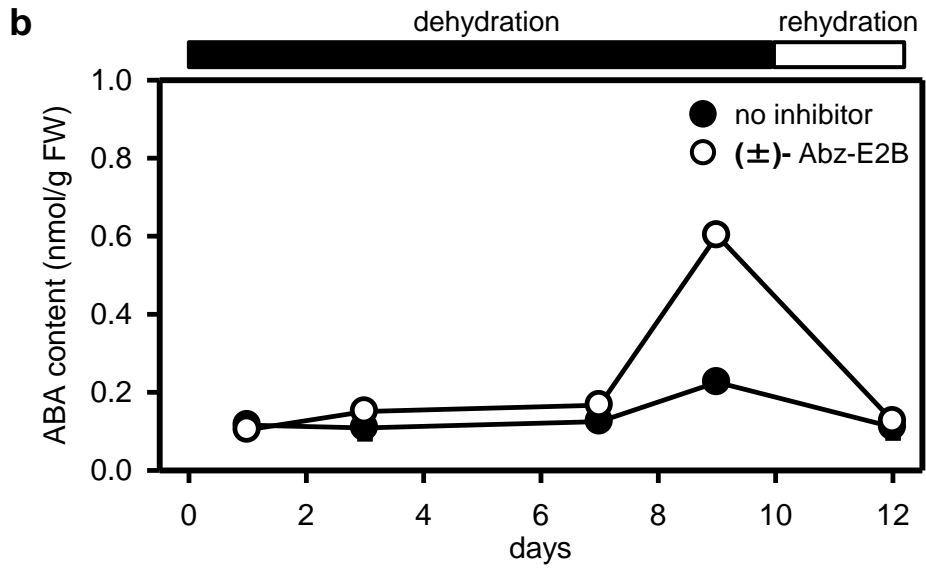
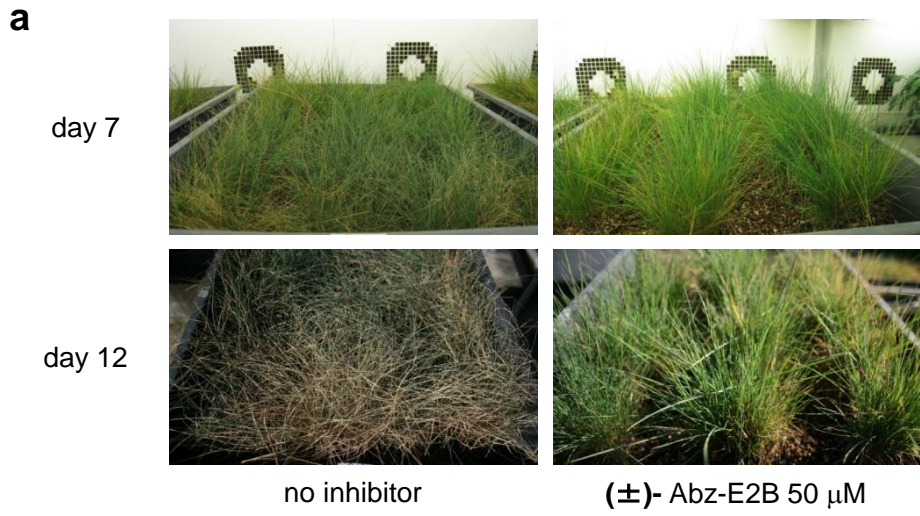


Figure 4

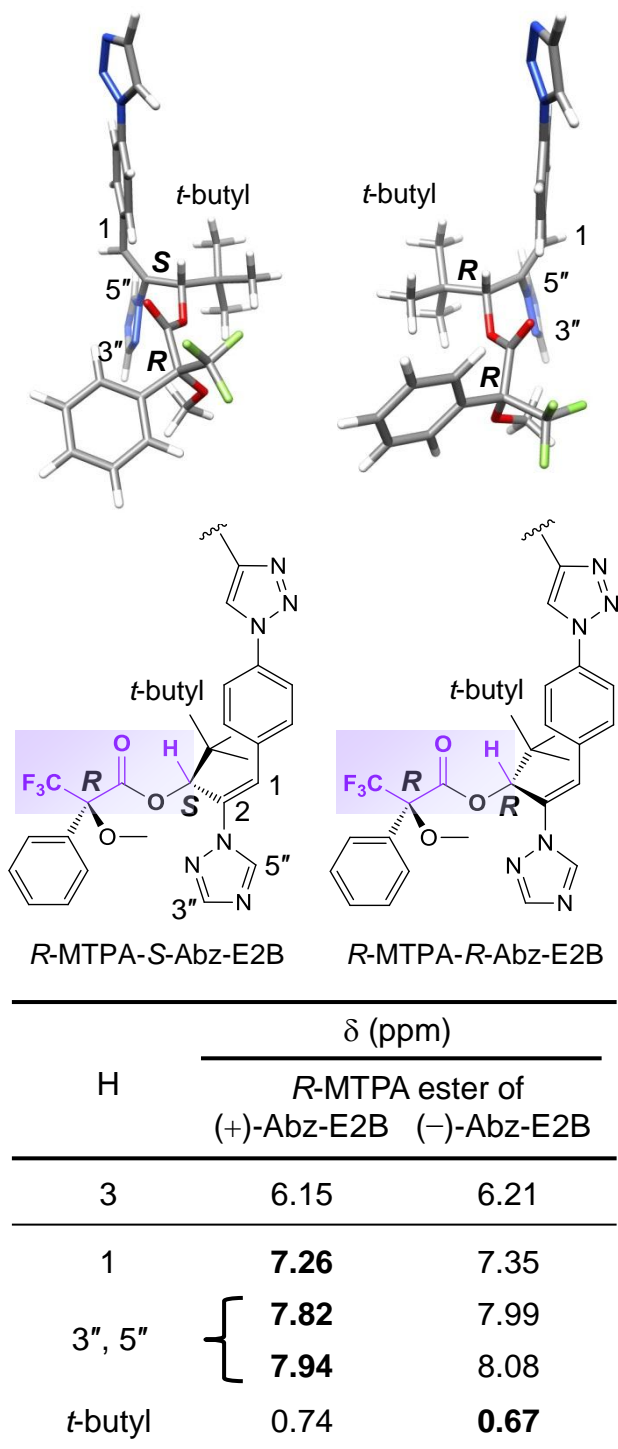


Figure 5

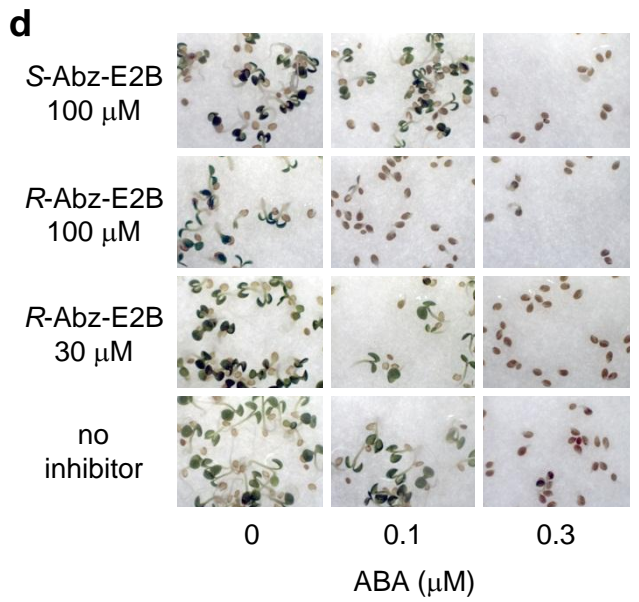
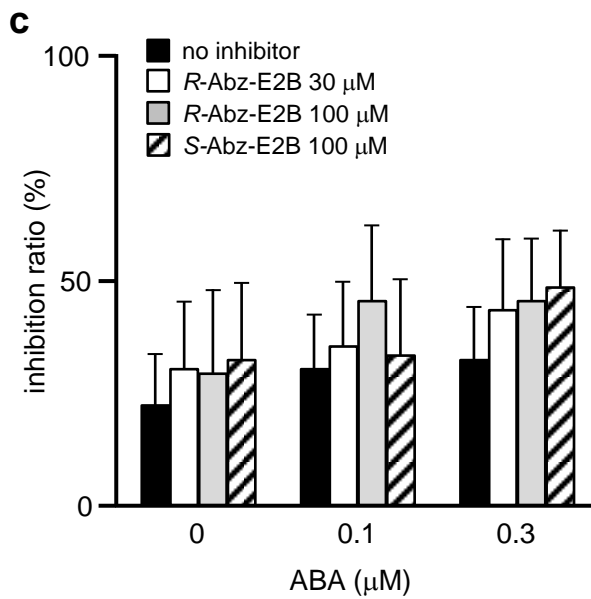
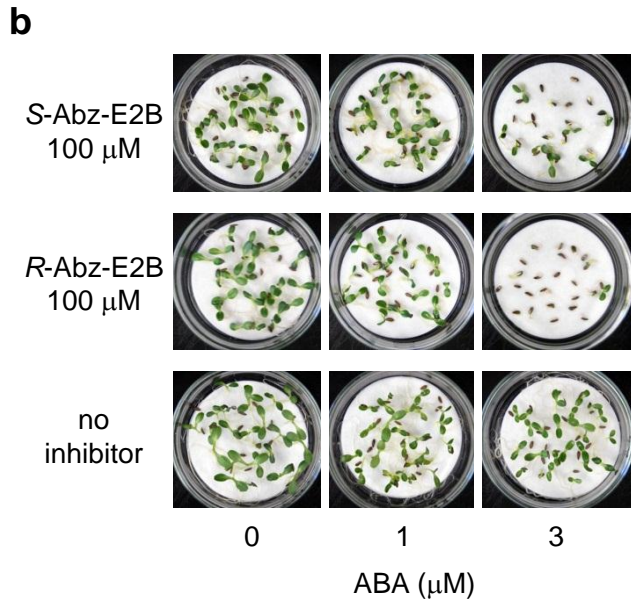
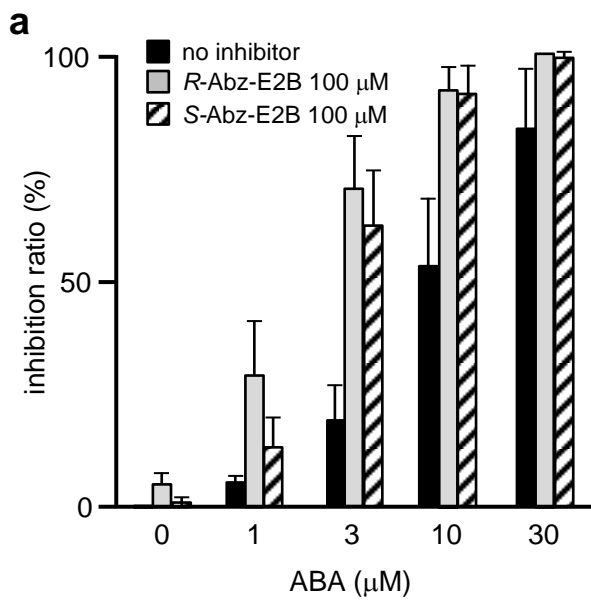


Figure 6

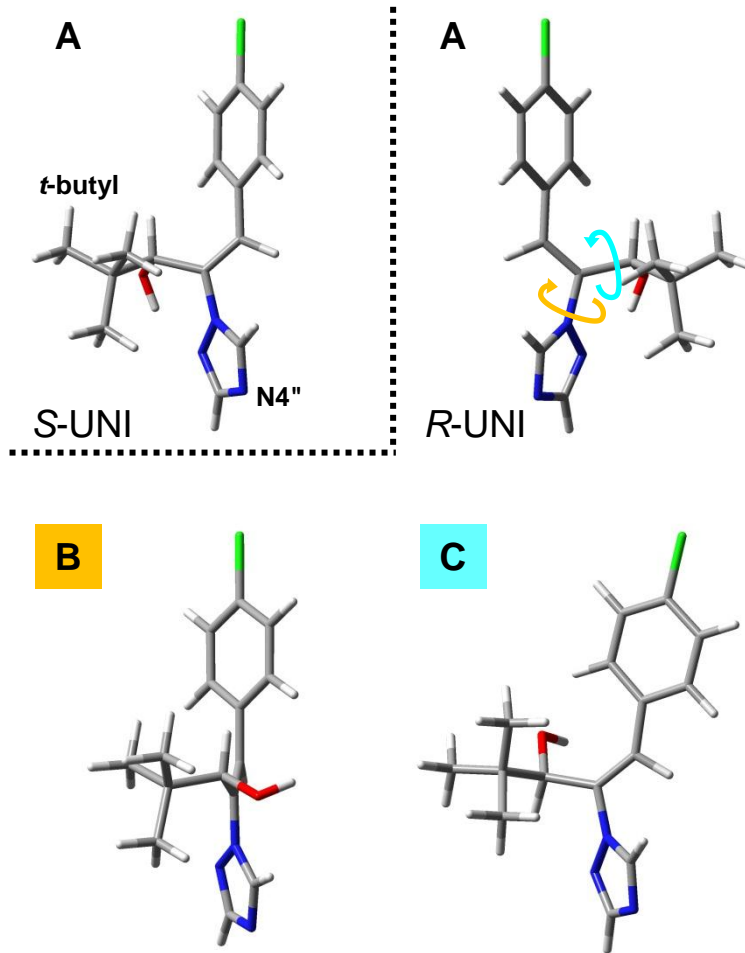
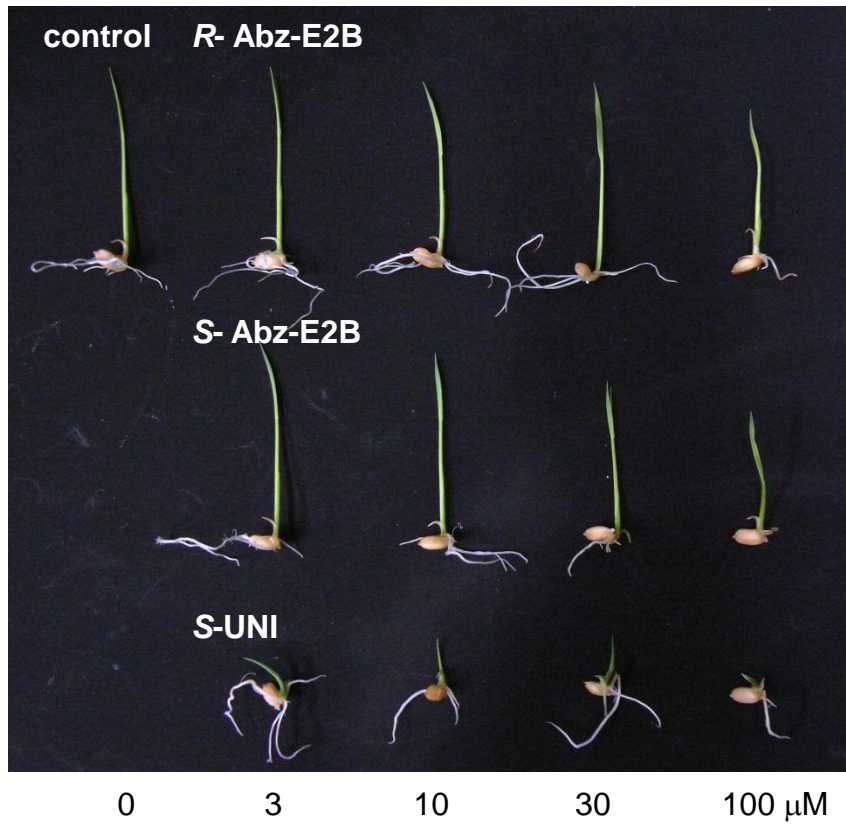


Figure 7

a



b

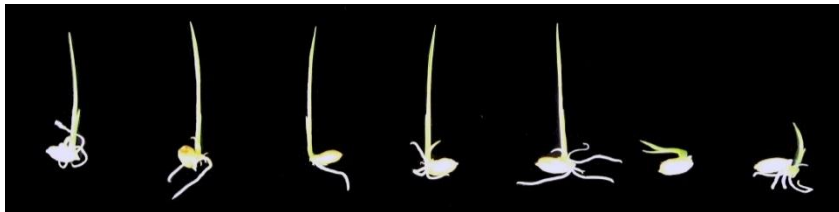


Figure 8

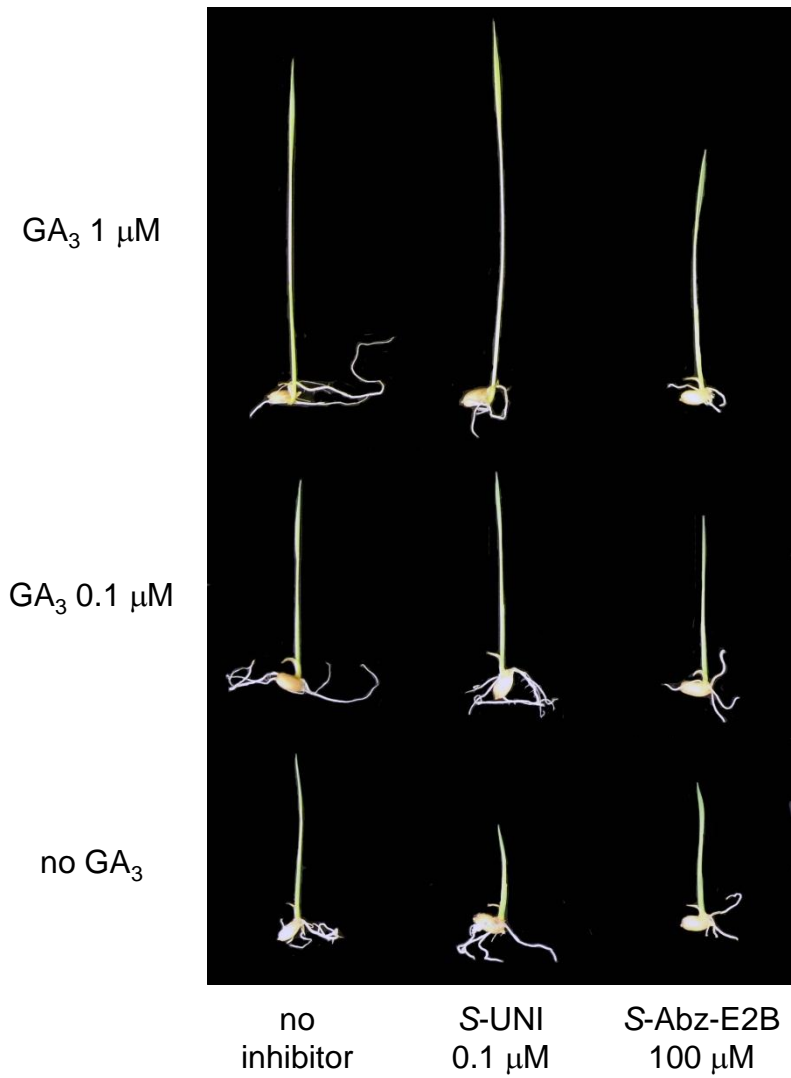
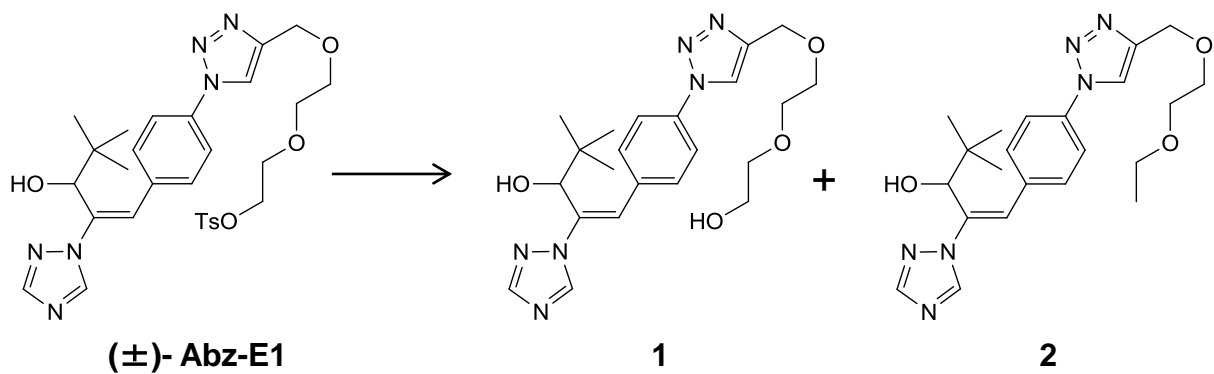
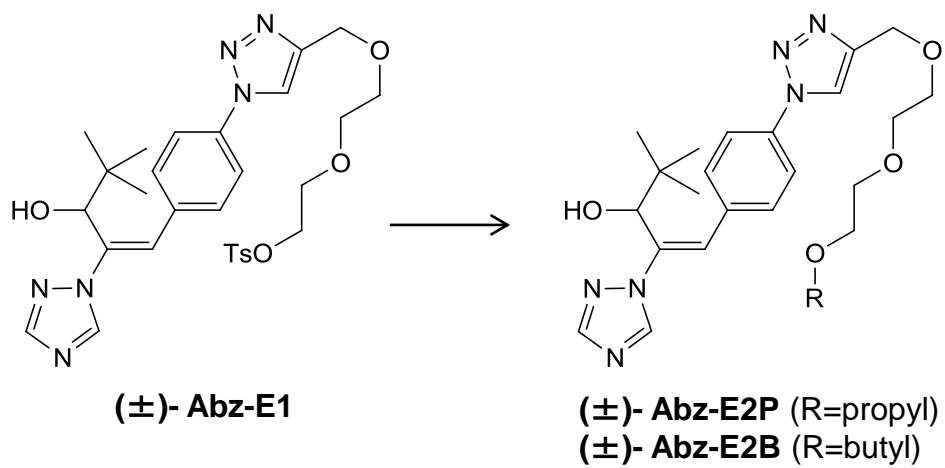


Figure 9



Scheme 1



Scheme 2